Cryogenically cooled bent double-Laue monochromator for high-energy undulator X-rays (50–200 keV)

S. D. Shastri,* K. Fezzaa, A. Mashayekhi, W.-K. Lee, P. B. Fernandez and P. L. Lee

Advanced Photon Source, Argonne National Laboratory, Argonne, IL 60439, USA. E-mail: shastri@aps.anl.gov

A liquid-nitrogen-cooled monochromator for high-energy X-rays consisting of two bent Si(111) Laue crystals adjusted to sequential Rowland conditions has been in operation for over two years at the SRI-CAT sector 1 undulator beamline of the Advanced Photon Source (APS). It delivers over ten times more flux than a flat-crystal monochromator does at high energies, without any increase in energy width ($\Delta E/E \simeq 10^{-3}$). Cryogenic cooling permits optimal flux, avoiding a sacrifice from the often employed alternative technique of filtration – a technique less effective at sources like the 7 GeV APS, where considerable heat loads can be deposited by high-energy photons, especially at closed undulator gaps. The fixed-offset geometry provides a fully tunable in-line monochromatic beam. In addition to presenting the optics performance, unique crystal design and stable bending mechanism for a cryogenically cooled crystal under high heat load, the bending radii adjustment procedures are described.

Keywords: X-ray optics; high-energy X-rays; high-energy monochromators.

1. Introduction

Recent third-generation synchrotron sources based on storage rings operating at high electron beam energies (6–8 GeV) produce intense radiation in the form of high-energy X-rays that are well suited to specific applications in materials and physics research (Schneider, 1995; Suortti, 1997). Development of efficient optics, such as monochromators, for X-rays of short wavelengths under 0.25 Å becomes a necessity. The standard double-crystal monochromator consisting of two flat perfect parallel crystals [*e.g.* Si(111) in a non-dispersive setting] is ideal for most low-energy experiments (under 30 keV), but not for high energies (over 50 keV). Although this concept fundamentally still works, it does not extract photons from the white beam in an efficient manner, as clarified below. In this article, an alternative monochromator optics scheme, composed of two bent Laue crystals, is described that efficiently delivers monochromated high-energy synchrotron radiation. Such optics has been tested and is routinely used in the 50–100 keV range at the SRI-CAT 1-ID undulator beamline of the Advanced Photon Source (APS). It provides over ten times more flux in the same monochromatic output energy width as flat Bragg crystals and is characterized by a fully tunable fixed-exit beam with preserved source brilliance (divergence and size). This bent double-Laue scheme for high photon energies is presented here with a description of its performance, crystal design, bending mechanism, cryogenic cooling and bending adjustment procedure.

The profound contrast in the level of efficiency of a flat Si(111) double-crystal monochromator, depending on whether it is set to select 10 keV or 100 keV from a white beam, is illustrated by the Dumond representations in Fig. 1 for the case of an APS undulator A source. Dumond diagrams offer a convenient graphical means of visualizing the evolution of the two-dimensional distribution, in angle and energy, of a ray-ensemble of photons undergoing multiple Bragg reflections through a sequence of flat perfect crystals (Dumond, 1937). In the 10 keV case, the monochromator roughly selects all the white-beam radiation within an energy range $\Delta E/E \simeq 1.4 \times 10^{-4}$. However, when the energy is increased to 100 keV, the Bragg angle θ and angular acceptance (Darwin width) decrease significantly. The steep narrow acceptance slice arising from the small Bragg angle and narrow Darwin width results in a fairly large energy width in the monochromated beam ($\Delta E/E \simeq 2 \times 10^{-3}$) but without the benefit of maximum flux. Over 90% of the radiation in the white beam within that energy width *does not* pass through the optics. In addition to the Si(111) reflection properties at 100 keV, this inefficient performance is also exacerbated by the enlarged vertical divergence (53 µrad) from the source at high energies and closed-gap operating conditions. Unlike at lower energies (under 50 keV), where the divergence is governed by the particle beam's small emittance ($2.35\,\sigma_{y'} \simeq 9$ µrad), at high energies the insertion-device field errors and particle-beam energy spread give rise to somewhat wiggler-like behavior (Shastri *et al.*, 1998) and hence larger vertical divergences of order $1/\gamma$, where γ is the relativistic parameter. The APS undulator A is a 3.3 cm-period device with 70 planar periods and a deflection parameter $k = 2.7$ at

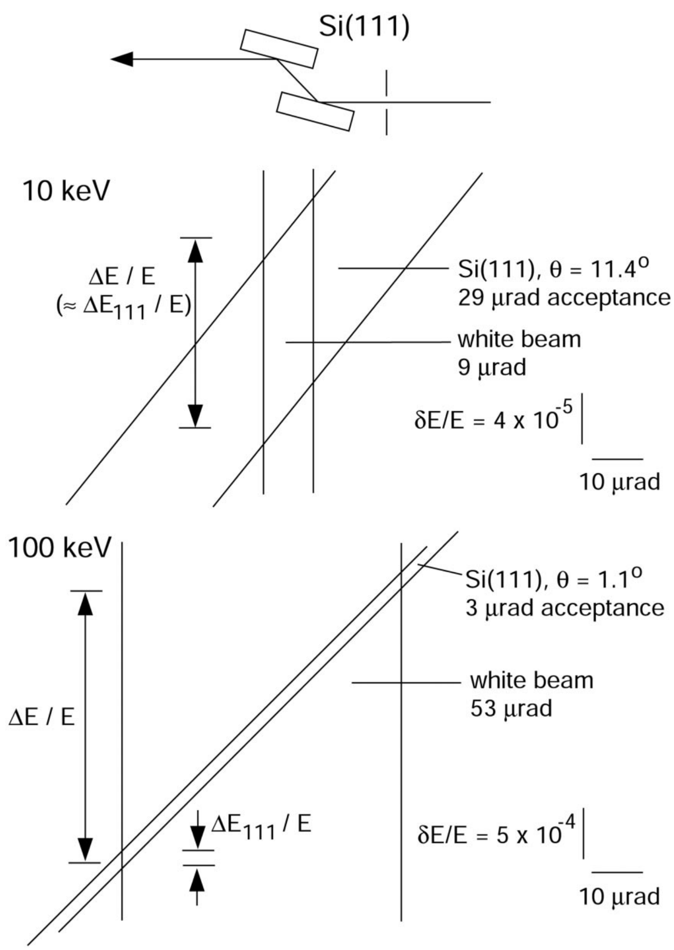

Figure 1
Dumond diagram representations of a flat Si(111) monochromator set for 10 keV and 100 keV in an APS undulator A white beam. Note that the vertical energy scale $\delta E/E$ is over 12 times more compressed in the 100 keV case to accommodate the steep crystal acceptance slice. Extents of the total energy spread $\Delta E/E$ and intrinsic crystal bandwidth $\Delta E_{111}/E$ are indicated.

the minimum 11 mm gap, operating in a 7 GeV electron storage ring (Lai *et al.*, 1993; Dejus *et al.*, 1994).

2. Bent double-Laue geometry

To improve on the flat-crystal optics for the 100 keV case just discussed, one could attempt to develop a method that leaves the monochromated energy width unchanged but enhances flux by over a factor of ten by passing through all the photons from the source within that $\Delta E/E \simeq 2 \times 10^{-3}$ bandwidth. Such a bandwidth is acceptable for numerous high-energy experiments currently performed at sector 1 of SRI-CAT, such as pair-distribution function measurements (Petkov *et al.*, 2000; Badyal *et al.*, 1997), fluorescence spectroscopy (Curry *et al.*, 2001), powder diffraction (Wilkinson *et al.*, 2002; Kramer *et al.*, 2002) and material stress/texture determination (Almer *et al.*, 2002). In order to achieve the desired enhancement in output, one must increase the narrow angular acceptance of crystals at high energies. That significant diffracted-flux increases of one to two orders of magnitude are attainable by bending perfect crystals, thereby strain-broadening their angular acceptances, has already been pointed out and investigated for high-energy X-ray optics (Suortti *et al.*, 1994; Suortti & Schulze, 1995). Bent-crystal dynamical diffraction calculations show that asymmetrically cut Laue crystals are well suited for use in this fashion, as the degree of broadening of the reflectivity curve can be finely controlled by the choice of thickness, asymmetry angle and bending radius parameters. However, an increase in the angular width of a crystal's reflectivity curve at fixed energy is accompanied by an undesired increase in the energy acceptance at fixed angle. Fortunately, one can mitigate this effect of enlarged diffracted-beam energy spread by bending the crystal towards the source, with a bend radius properly adjusted so that all rays from the source make the same incidence angle with respect to the crystal planes (the so-called Rowland condition), as elaborated below. Employing these ideas by adopting the bent double-Laue configuration, depicted in Fig. 2, accomplishes the desired improvement in output. The white beam is incident on the first Laue crystal, cylindrically bent to a Rowland circle going through the source *S*1. The singly diffracted beam emerges as if emanating directly from a virtual source *S*2, also located on the first Rowland circle. To restore the beam parallel to the original direction and provide a tunable in-line system, a second crystal is introduced and is also bent, but to a Rowland circle going through the virtual source *S*2. The doubly diffracted beam propagates as if coming from the virtual source *S*3 located on the second Rowland circle and close to the original source *S*1. The setting of a Laue crystal to a Rowland condition is also known as the inverse-Cauchois geometry. Such a bent double-Laue concept has already been employed previously for tomography applications (Ren *et al.*, 1999).

The over tenfold flux increase results from the bending strain-induced broadening of the crystal reflection's angular acceptance, as shown in Fig. 3. The intrinsic acceptance $\Delta\theta_{\rm acc}$ changes from 3 µrad in the flat Bragg case to 40 µrad in the asymmetric bent Laue case, thereby enabling efficient monochromatization. [The Laue reflectivity curve was calculated using the bent-crystal dynamical diffraction computer code *PEPO* (Schulze & Chapman, 1995).] Despite this broadening, one does not suffer any additional detrimental energy width because the spread of angles of incidence $\Delta\theta_{\rm inc}$ with respect to the crystal lattice decreases from 53 µrad in the flat Bragg case to 1.6 µrad in the bent Laue case. This near vanishing of $\Delta\theta_{\rm inc}$ is characteristic of the Rowland geometry, which makes all rays from any given point within the source impinge at the same angle onto the bent-crystal lattice, leaving only a small source-size contribution. The net result leaves the total energy spread $\Delta E/E = \cot\theta\,(\Delta\theta^2_{\rm acc} + \Delta\theta^2_{\rm inc})^{1/2}$ essentially unchanged from 2.5×10^{-3} to 2.0×10^{-3} in going from flat Bragg to bent Laue geometries at 100 keV.

Widened angular acceptances also result when bending perfect Bragg crystals or when using mosaic crystals. However, unlike the Laue geometry where one is operating near normal incidence, the grazing-incidence situations encountered with Bragg crystals lead to very large ($\sim$ km) bending radii for the Rowland condition, providing insufficient lattice strains for significant acceptance enhancements. Mosaic crystals are not the superior choice for two reasons. First, the preservation of high flux through two mosaic reflections is a concern, although it is more likely to be successful at high energies where the long penetration lengths help the probability of 'mosaic crystallite matching' between the two crystals. Second, the preservation of brilliance (*i.e.* beam divergence and size) is questionable, although here again one could argue that in a two-crystal setup there is, for a given ray, an inherent selection property that picks parallel mosaic crystallite pairs in the double-reflection process that should limit the

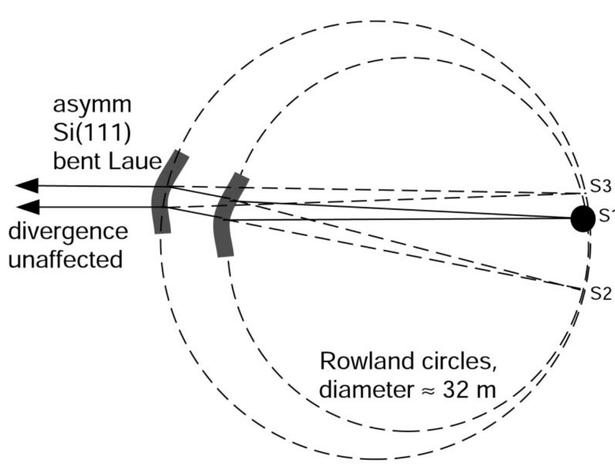

Figure 2
Tunable in-line monochromator of two vertically diffracting bent Laue crystals located at about 32 m from the undulator source *S*1. The two Rowland circles intersect tangentially at the virtual source *S*2.

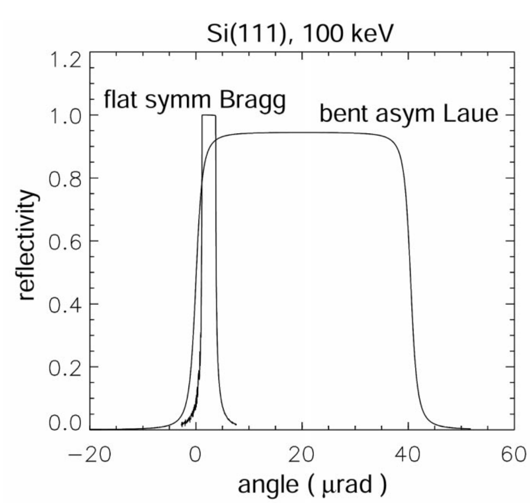

Figure 3
Dynamical diffraction calculations for 100 keV X-rays of intrinsic Si(111) reflectivities for the flat symmetric Bragg and bent asymmetric Laue cases. The latter case assumes a 32 m bend radius, 10° asymmetry and 2.5 mm thickness.

beam-divergence increase. Nevertheless, a beam-size blow-up effect can still arise owing to the crystal depth uncertainty of the diffraction phenomenon. In the bent double-Laue approach using perfect crystals, the preservation of flux and brilliance is clear and experimentally verified. One must point out that in a single bent Laue-reflection geometry, there is indeed a slight strain- and thickness-induced beam enlargement. However, for the double-Laue-reflection setup, a nearly complete compensation effect between the two identically oriented and bent crystals suppresses the beam expansion (Lienert *et al.*, 2001). Hence, this configuration promises possibilities of further beam manipulation with coherence-prerequisite optics such as stacked Fresnel zone plates (Shastri *et al.*, 2001) and compound refractive lenses (Snigirev *et al.*, 1996; Lengeler *et al.*, 1999) for focusing or collimation.

3. Design aspects

The heat-load challenge for high-energy X-ray optics with insertion-device sources is often met by filtration, whereby absorbers are placed in the white beam to preferentially attenuate the low-energy X-rays, without imposing a substantial sacrifice of the desired high-energy photons. The goal in such a scheme is to alleviate the thermal load on the first crystal enough to render a simple water-cooling system sufficient. However, this method was not used for the optics described here. Instead, liquid-N_2 cooling was employed for two reasons. First, the cryogenic pumping systems were readily available owing to their earlier development and routine use for flat-crystal monochromators operating at lower energies (Lee *et al.*, 2000). The more important second reason is that, for sources like undulator A operating at minimum gap in a 7 GeV storage ring, the power carried and deposited by high-energy photons is substantial and ever-increasing in view of future upgrades to doubled undulator lengths and higher ring currents. In reducing thermal loads to water-cooling levels by using aluminium or copper filters, one encounters unacceptable flux reductions that, depending on the high energy of interest, can range anywhere from a factor of two at best to over an order of magnitude. However, a 1.5 mm graphite absorber was used here to remove some power from low-energy (few keV) X-rays while still leaving the transmission of high-energy photons (>50 keV) close to unity.

Of technical importance in implementing the bent double-Laue monochromator optics is achieving fine control and stability of the bend radii of the two silicon crystals. The first crystal, in particular, poses additional difficulties because of the presence of harsh non-equilibrium conditions of closed undulator-gap heat load and cryogenic cooling. Crystal benders providing the required mechanical control and stability were developed that operate by inducing the cylindrical deflection of a stiff triangular crystal by pushing indirectly on its tip through a weak spring, as sketched in Fig. 4. In this way, a large input displacement (millimeters) at one end of the spring results in a small deflection (micrometers) at the other end, *i.e.* the crystal tip. Owing to the constant well defined applied force, the crystal settles into a well defined bend radius that is stable against mechanical shocks, thermal drifts or mechanical creep anywhere in the system, thereby freeing one from readjusting the benders for months at a time. The invariance of the elastic constants of silicon over the temperature range of interest gives an unchanging bend radius despite the possibility of crystal temperature changes. A cylindrical bend without transverse twisting from anisotropic elastic constants is attained by cutting the crystal in a crystallographic orientation so that the plane perpendicular to the crystal and containing the altitude line of the isoceles triangle forms a mirror plane of the diamond-cubic structure.

For both crystals, the triangular leaf is 5 mm thick throughout, except at the large base, which is clamped between the two metal blocks, and at the spot of beam incidence, which is thinned down (by ultrasonic drilling) to the desired diffraction thickness of 2.5 mm over a small circular region (see Fig. 4). The reasons for having the crystal overly thick everywhere except at the diffracting area are threefold. First, this gives it the overall stiffness appropriate to the applied bending forces and desired stability. Second, using another crystal with different diffraction thickness but the same overall thickness does not require readjustment of the bender (*i.e.* changing springs). Finally, for the first crystal under heat load, the extraction of deposited heat is facilitated by the presence of the thicker surrounding region. The depth positioning of the thin diffracting section within the overall 5 mm thickness of the main wafer (*e.g.* whether symmetrically centered or offset to be flush with the main surface) has no observable influence on thermal performance. The cryogenic cooling for the first crystal is accomplished by flowing liquid N_2 through the copper blocks clamping the base and by a thin layer of In–Ga eutectic to provide good heat transfer across the silicon–copper interfaces. One of the main reasons for the large base-block section as part of the silicon crystal geometry was to permit the option of later drilling a cooling channel path through there in order to have cryogenic flow directly within the silicon. This, however, has not yet been tested.

4. Performance

This section addresses the performance of the optics with regard to flux, energy resolution, energy drift stability and brilliance preservation. Table 1 summarizes the flux and energy-width results for three energies (67, 75 and 100 keV) at which the bent double-Laue Si(111) scheme was tested. As measured by a calibrated N_2-gas-filled ioni-

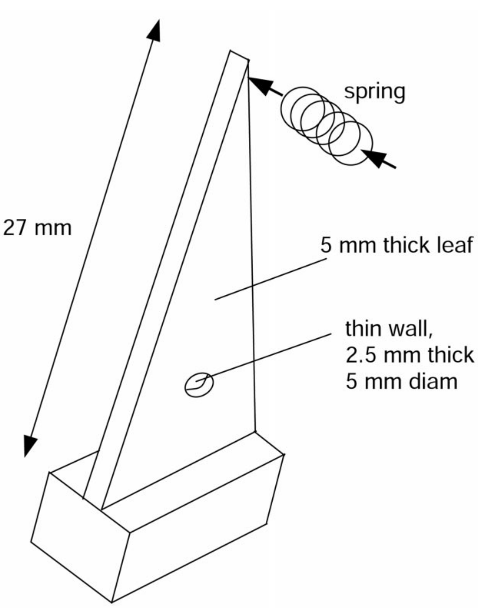

Figure 4
Sketch of triangular silicon Laue crystal. The applied spring force cylindrically bends the leaf, including the thin wall where the beam diffracts. The first monochromator crystal is clamped at the large base section between two liquid-N_2-cooled copper blocks (not shown).

Table 1
Measured bent Laue monochromator fluxes and energy resolutions at 67, 75 and 100 keV.

Calculated resolutions are also given for both the flat Bragg and bent Laue cases, showing essentially no changes in energy spread. Performance at 210 keV was also studied (see text).

Photon energy (keV)	Undulator gap (mm)	Flux at 100 mA, 1 × 1 mm slits at 27 m (photon s^{-1})	Energy resolution $\Delta E/E$ ($\times 10^{-3}$) Flat calculated	Bent calculated	Bent measured
67	11.215	1.2×10^{13}	1.3	1.4	1.4
75	11.212	1.0×10^{13}	1.4	1.5	1.6
100	11.000	6.3×10^{12}	1.9	2.0	2.0

zation chamber, the monochromatic flux delivered in a beam defined by a 1 × 1 mm white-beam aperture placed 27 m from the source ranged from 1.2×10^{13} photons s^{-1} (at 67 keV) to 6.3×10^{12} photons s^{-1} (at 100 keV) for 100 mA ring current and 11.0 mm undulator gap. The measured energy spreads $\Delta E/E$ at 67, 75 and 100 keV were 1.4×10^{-3}, 1.6×10^{-3} and 2.0×10^{-3}, respectively, in exact agreement with calculations and comparable to that which flat Si(111) optics would give at less than one-tenth the flux under the same operating conditions of current, gap and slits. The energy width of the monochromated beam was determined by the angular scanning of an additional flat Si analyzer crystal through the high-order 777 reflection (Fig. 5). The monochromator was also tested at the very high energy of 210 keV, for which the flux was 5.3×10^{10} photons s^{-1} when diffracting through the thin 2.5 mm sections of both crystals and 1.0×10^{11} photons s^{-1} when diffracting through the thick 5 mm sections, with relative energy spreads of 0.006 and 0.008, respectively.

Energy-drift stability is an important consideration in high-energy X-ray optics as the low Bragg angles amplify small angular instabilities of thermal/mechanical origin into large energy shifts. For example, a 1 arcsec ($\sim 4.8\,\mu$rad) angular shift of an Si(111) crystal corresponds to an energy shift of only 0.24 eV at 10 keV (*i.e.* 2.4×10^{-5}), but 25 eV at 100 keV (*i.e.* 2.5×10^{-4}). During the last two years of operation of the optics, the energy stability was regularly investigated and gradually improved. The energy drifts were monitored over long periods (a few hours to a couple of days, sometimes in parallel with independent experimental data acquisition) by tuning the monochromator to the center of the steep Au *K* absorption edge at 80.725 keV and continuously recording the transmission through a thin Au foil. With refinements in the mechanical details of the first crystal stage and operating parameters of the liquid-N_2 pump, energy drifts were improved from excursions of ±30 eV to better than ±5 eV (*i.e.* < 10^{-4}). The significant step in improvement came as a consequence of upgrading the cryogenic pump to a model version designed to minimize pressure perturbations in the closed-loop system arising from the intermittently refilled heat exchange bath.

The claim that the optics leave the ray propagation from the source undisturbed was verified to a reasonable level by comparing horizontal and vertical beam profiles at different locations and examining whether the sizes scaled with the distances from the source. Setting the white-beam slits positioned at 27 m to define a square aperture of dimensions 0.8 × 0.8 mm produced monochromatic beam sizes of 1.1 × 1.1 mm at 35 m and 1.7 × 1.7 mm at 58 m, in exact agreement with the distance ratios. This simple test is evidence of ray divergence preservation at the few microradian level and has been supported by the successful collimation of the monochromated beam by compound refractive lenses at 81 keV (Shastri, 2002).

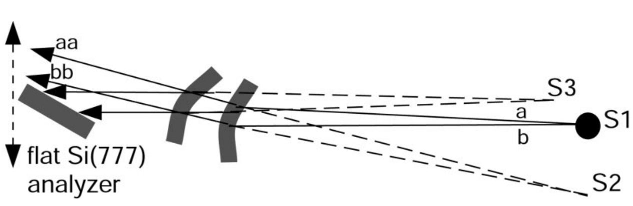

Figure 5
A flat Si(777) analyzer crystal after the monochromator measures the energy width of the final exit beam. Raising the analyzer to intercept the singly reflected beam (rays 'aa', 'bb') aids the first crystal's adjustment to the correct curvature.

5. Bending radii adjustment

This section is devoted to the important operational matter of proper adjustment of both crystals' bend radii so as to attain the desired monochromator performance. Tuning the first crystal's curvature to the Rowland condition is performed with the assistance of an auxiliary flat-crystal analyzer, as shown in Fig. 5. This crystal, set to the vicinity of the high-order Si(777) Bragg reflection, is shown in that figure intercepting the beam after double reflection by both Laue crystals, just as it would be set up to measure the energy spread of the final monochromatic beam. However, to enable determination of the correct bending radius of the first crystal, the analyzer is translated vertically away from the position shown to intercept the singly diffracted monochromatic beam from the first Laue crystal (*i.e.* the rays labeled 'aa', 'bb'). In this configuration, the second Laue crystal is either displaced out of the way or left in the beam – but rotated off its Bragg condition to transmit the X-rays. The white-beam slits, located 27 m from the source, define a vertically fine beam aperture (1.5 mm horizontal, 0.1 mm vertical) and select rays passing either 0.75 mm above or 0.75 mm below the undulator axis (*i.e.* the beam center) depending on where they are placed. When positioned 0.75 mm above the axis, the ray 'a' is selected and then deflected by the first crystal into ray 'aa' going towards the analyzer. Similarly, when the aperture is positioned below the axis, ray 'b' is isolated and then diffracted by the first crystal towards the analyzer as 'bb'. Si(777) analyzer rocking curves are taken for both above- and below-axis rays. This pair of rocking curves is repeated for various bender settings (*i.e.* spring pusher positions) of the first crystal. The results of such a procedure are displayed in Fig. 6. The high-order analyzer angular scans effectively serve as a spectral profile measurement of the incident radiation. The significant broadening of the reflection with more curvature is consistent with the principle mentioned earlier of acceptance increase due to bending strain. More relevant here, however, is the merging and eventual crossing of the peak centroid positions $\overline{\theta}_{777,\rm bb}$ and $\overline{\theta}_{777,\rm aa}$. This is presented slightly differently in Fig. 7, which plots the peak separation $\overline{\theta}_{777,\rm bb} - \overline{\theta}_{777,\rm aa}$ (*i.e.* below axis minus above axis) as a function of pushing/bending. The bender setting at which the centroid separation vanishes is close to the Rowland condition for the first crystal, as it indicates that nearly the same energy is diffracted above and below the axis because all the white-beam rays make almost the same incident angle onto the curved lattice. In the preceding statement, one is careful to state that the zero-crossing bend radius corresponds to being near, but not precisely at, the Rowland condition. This is because even when rays 'aa' and 'bb' do indeed have the same energy, they come in at incident angles with respect to the analyzer that are slightly different by an amount given by the angle subtended by the white-beam slits' vertical motion about the source, which in this case is $(2 \times 0.75\,\text{mm})/(27\,\text{m}) = 56\,\mu\text{rad} = 0.003^\circ$. So, as indicated in Fig. 7, the exact Rowland condition is attained slightly past (*i.e.* additional bending beyond) the centroid crossing, where the peak splitting is $\overline{\theta}_{777,\text{bb}} - \overline{\theta}_{777,\text{aa}} = -0.003^\circ$.

After the curvature of the first crystal is set, adjusting the second Laue crystal's bending radius is straightforward and does not involve the analyzer. One simply orients the second crystal to the Bragg reflection and measures the peak intensity of the doubly reflected beam as a function of its bending (Fig. 8). As the second crystal's acceptance increases, the intensity climbs rapidly and then abruptly levels off when the two bent crystals are just matched in acceptance. This procedure is performed with a large vertical beam size (here 0.1 mm horizontal, 2 mm vertical) for sensitivity to mismatched curvatures. The saturation intensity is approximately 20 times the starting flat-crystal value, consistent with the known facts that there should be a twofold gain in going from the flat Laue to a flat Bragg geometry and a tenfold gain in going from a flat Bragg to the bent Laue configuration (Fig. 3). As indicated in Fig. 8, the Rowland condition for the second crystal is achieved at the bending setting where the exit beam intensity stops increasing. Beyond this curvature, the width of the second crystal rocking curve increases significantly, without introducing more intensity, manifesting an over-bent state.

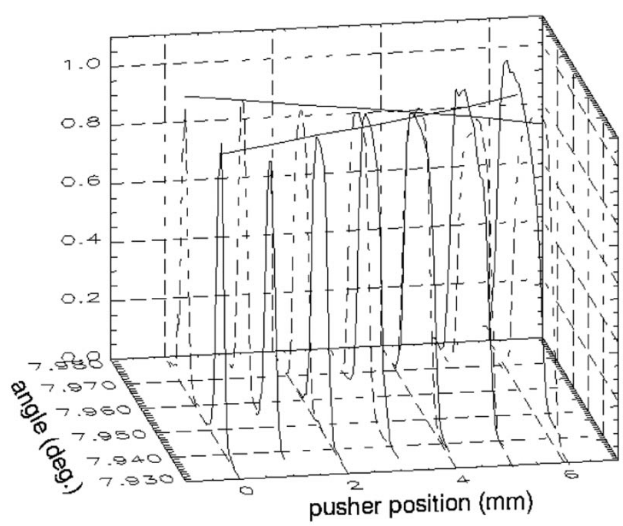

Figure 6
Si(777) analyzer rocking curves taken in the singly reflected beam for varied first-crystal bending, with above-axis (solid curves) and below-axis (dashed curves) rays. Intersecting lines show the centroids crossing near the Rowland condition.

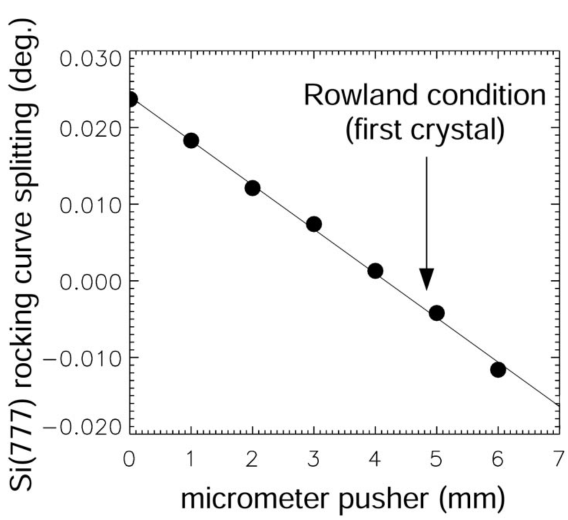

Figure 7
The separation $\overline{\theta}_{777,\text{bb}} - \overline{\theta}_{777,\text{aa}}$ between the centroids of analyzer rocking curves (from Fig. 6) taken above and below axis as a function of first-crystal bending.

6. Concluding remarks

The bent double-Laue monochromator at the APS 1-ID undulator beamline is a fully tunable in-line system that efficiently delivers high-energy monochromatic beams. Although its energy resolution is modest ($\Delta E/E \simeq 10^{-3}$), it is no worse than that from a flat-crystal monochromator (Table 1) and provides over an order of magnitude more flux. The choice of bent perfect crystals over mosaic crystals results in a high degree of brilliance preservation. A unique crystal design allows cryogenic cooling and bending. Liquid-N_2 cooling frees one from white-beam filtration schemes and results in no intensity sacrifice. The stable bending mechanisms require no readjustment for months at a time, even for the first crystal facing closed undulator-gap heat load and cryogenic cooling perturbations.

Strictly speaking, the claim that the new optics offer over tenfold more flux in the same energy width than conventional flat Si(111) crystals is valid for the insertion device used here and for the typical 1 mm vertical aperture placed 27 m from the source. Reducing the vertical angular aperture clearly decreases the flux delivered from both systems by the same factor. However, the energy resolution from the flat crystals improves, whereas that from the bent double-Laue optics remains unchanged. This disparity in the influence on the energy resolution would also be present if a narrower vertical divergence is imposed by the use of an insertion device optimized for high-energy X-rays, *i.e.* one with low-order odd harmonics tunable through the 50–100 keV range and with small beam divergence determined by the particle beam emittance. Although undulator A is quite a high-brilliance source at high photon energies, it is not fully optimized for that energy range in the sense just mentioned. When working over 50 keV, one uses this device with a minimum gap setting and operates in the spectral region where the high-order harmonics are smeared out due to field errors and electron energy spread,

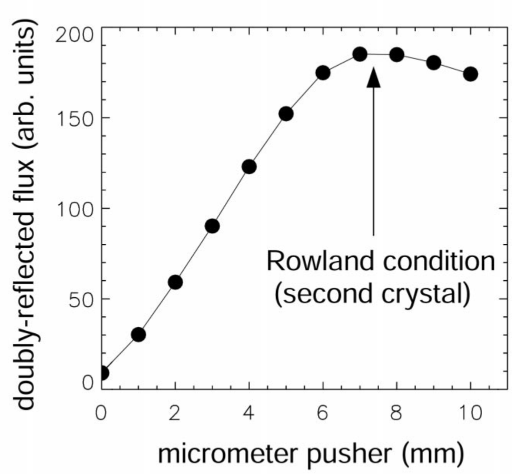

Figure 8
Variation of the exit intensity from the double-Laue monochromator as a function of second-crystal bending.

resulting in wiggler-like source behavior with larger divergences of order $1/\gamma$ (Shastri *et al.*, 1998).

Although 10^{-3} energy resolution in the 50–100 keV range is sufficient for most high-energy experiments presently conducted at the 1-ID beamline, *e.g.* pair-distribution function measurements, fluorescence spectroscopy, powder diffraction and material stress/texture determination, one sometimes requires better monochromaticity. The energy resolution can be improved to 10^{-4} levels or better by careful choice of Laue-crystal parameters such as thickness, asymmetry and reflection order. However, higher resolutions at high X-ray energies demand excellent stability, which is difficult to achieve at the white-beam optics stage. So, attaining energy resolutions narrower than 10^{-4} might be best achieved alternatively using additional post-monochromatization optics after the broader-bandwidth double-Laue system described. For example, compound refractive lenses can collimate the exit beam to divergences within the small angular acceptances of subsequent high-resolution flat-crystal optics, as suggested by Baron *et al.* (1999), who examined compound refractive lenses as collimators at lower energies. This method would require a pre-monochromator that is brilliance preserving – a feature inherent in the bent double-Laue concept. Horizontal focusing can be incorporated into the optics by bending the asymmetric Laue crystals sagittally, as well as meridionally, by exploiting the anticlastic bending phenomenon (Zhong *et al.*, 2001*a*,*b*). This approach has been demonstrated successfully to focus the wide horizontal radiation fan from a bending-magnet source. However, it might be of value even for undulator sources, which can emit with a substantial horizontal divergence at high energies because of device field errors and particle-beam energy spread.

The crystals were fabricated by R. Khachatryan and thermal engineering assistance was provided by G. Tajiri and D. Ferguson. Use of the APS was supported by the US Department of Energy, Office of Science, Basic Energy Sciences, under Contract No. W-31-109-Eng-38.

References

Almer, J., Lienert, U. & Haeffner, D. R. (2002). In preparation.

Badyal, Y. S., Saboungi, M.-L., Price, D. L., Haeffner, D. R. & Shastri, S. D. (1997). *Europhys. Lett.* **39**, 19–24.

Baron, A. Q. R., Kohmura, Y., Ohishi, Y. & Ishikawa, T. (1999). *Appl. Phys. Lett.* **74**, 1492–1494.

Curry, J. J., Adler, H. G., Shastri, S. D. & Lawler, J. E. (2001). *Appl. Phys. Lett.* **79**, 1974–1976.

Dejus, R. J., Lai, B., Moog, E. R. & Gluskin, E. (1994). Report ANL/APS/TB-17. Argonne National Laboratory, Argonne, IL, USA.

Dumond, J. W. M. (1937). *Phys. Rev.* **52**, 872–883.

Kramer, M. J., Margulies, L., Goldman, A. I. & Lee, P. L. (2002). *J. Alloy Compd.* **338**, 235–241.

Lai, B., Khounsary, A., Savoy, R., Moog, E. & Gluskin, E. (1993). Report ANL/APS/TB-3. Argonne National Laboratory, Argonne, IL, USA.

Lee, W.-K., Fernandez, P. & Mills, D. M. (2000). *J. Synchrotron Rad.* **7**, 12–17.

Lengeler, B., Schroer, C., Tümmler, J., Benner, B., Richwin, M., Snigirev, A., Snigireva, I. & Drakopoulos, M. (1999). *J. Synchrotron Rad.* **6**, 1153–1167.

Lienert, U., Keitel, S., Caliebe, W., Schulze-Briese, C. & Poulsen, H. F. (2001). *Nucl. Instrum. Methods Phys. Res. A*, **467**, 659–662.

Petkov, V., Billinge, S. J. L., Shastri, S. D. & Himmel, B. (2000). *Phys. Rev. Lett.* **85**, 3436–3439.

Ren, B., Dilmanian, F. A., Chapman, L. D., Ivanov, I., Wu, X. Y., Zhong, Z. & Huang, X. (1999). *Nucl. Instrum. Methods Phys. Res. A*, **428**, 528–550.

Schneider, J. R. (1995). Editor. *International Workshop on Scattering Experiments with High-Energy Synchrotron Radiation.* Hamburg: HASYLAB/DESY.

Schulze, C. & Chapman, D. (1995). *Rev. Sci. Instrum.* **66**, 2220–2223.

Shastri, S. D. (2002). In preparation.

Shastri, S. D., Dejus, R. J. & Haeffner, D. R. (1998). *J. Synchrotron Rad.* **5**, 67–71.

Shastri, S. D., Maser, J. M., Lai, B. & Tys, J. (2001). *Opt. Commun.* **197**, 9–14.

Snigirev, A., Kohn, V., Snigireva, I. & Lengeler, B. (1996). *Nature* (*London*), **384**, 49–51.

Suortti, P. (1997). Editor. *ESRF Workshop on High-Energy X-ray Scattering.* European Synchrotron Radiation Facility, Grenoble, France.

Suortti, P., Lienert, U. & Schulze, C. (1994). *Nucl. Instrum. Methods Phys. Res. A*, **338**, 27–32.

Suortti, P. & Schulze, C. (1995). *J. Synchrotron Rad.* **2**, 6–12.

Wilkinson, A. P., Lind, C., Young, R. A., Shastri, S. D., Lee, P. L. & Nolas, G. S. (2002). *Chem. Mater.* **14**, 1300–1305.

Zhong, Z., Kao, C. C., Siddons, D. P. & Hastings, J. B. (2001*a*). *J. Appl. Cryst.* **34**, 504–509.

Zhong, Z., Kao, C. C., Siddons, D. P. & Hastings, J. B. (2001*b*). *J. Appl. Cryst.* **34**, 646–653.

 Received 9 April 2002 • Accepted 5 June 2002